Tetra(2-oxopyridinato)chloroditechnitate. A New Compound with a Tc–Tc Bond of Order 3.5 and a Remarkable Vibronic Absorption Spectrum

F. Albert Cotton,* Phillip E. Fanwick, and Larry D. Gage

Contribution from the Department of Chemistry, Texas A&M University, College Station, Texas 77843. *Received July 30, 1979*

Abstract: The reaction of 2-hydroxypyridine (α-pyridone) with ammonium octachloroditechnitate (3.5) affords the insoluble title compound, which can be obtained as well-formed crystals by sublimation. The structure, established X-ray crystallographically, consists of infinite chains of $Tc_2(OC_5H_4N)_4^+$ units symmetrically linked by bridging Cl^- ions. The Tc–Tc distance is 2.095 (1) Å and the Tc–Cl distances are 2.679 (1) Å. Successful refinement was accomplished only in space group $I4/m$, treating each ligand as subject to a twofold orientational disorder. Unfortunately this makes it impossible to determine the point symmetry of an individual $[Tc_2(OC_5H_4N)_4]^+$ ion. The unit cell dimensions are a = 11.793 (3) Å, c = 7.454 (1) Å, and V = 1036.7 (6) Å^3, with Z = 2. There is a strong band in the Raman spectrum at 383 cm^{-1} that may be assigned to the "Tc–Tc" stretching mode and the compound has an ESR signal at a g value of 2.046. The electronic absorption spectrum has been examined in considerable detail using polarized crystal spectra recorded at 5 K. A general assignment is suggested and the rich vibrational structure of the $\delta^* \leftarrow \delta$ transition, whose 0–0 band is at 12 194.4 cm^{-1}, is fully assigned. This vibrational structure involves the participation of 11 vibrations. Its most remarkable feature is the occurrence, in z(Tc–Tc) polarization, of progressions involving ν(Tc–Tc), one totally symmetric ν(Tc–L), and all combination tones of these two vibrations.

Introduction

The chemistry of ditechnetium compounds with Tc–Tc bonds of high order has been remarkably limited considering how extensive is that of its closest neighbors, rhenium and molybdenum. One of the few such compounds known was discovered rather early, namely, $(NH_4)_3Tc_2Cl_8 \cdot xH_2O$, which was obtained by reduction of an HCl solution of TcO_4^- by zinc.[1] It has since been rather thoroughly characterized, as to both structure[2] and bonding.[3-5] The intriguing thing about the $[Tc_2Cl_8]^{3-}$ ion is, of course, the fact that, unlike $[Re_2Cl_8]^{2-}$, it has one more electron than the eight necessary to make a quadruple bond, with this "excess" electron occupying the δ^* orbital to give a $\sigma^2\pi^4\delta^2\delta^*$ configuration and a Tc–Tc bond order of 3.5. The exactly corresponding rhenium species, $[Re_2Cl_8]^{3-}$, has never been reported.

The preparation of compounds containing the $[Tc_2Cl_8]^{2-}$, perhaps by removal of one electron from the 3– ion, has been an obvious goal from the time the nature of $[Tc_2Cl_8]^{3-}$ was recognized,[2a] and electrochemical results[3] suggested that this ought to be a reasonable goal. In 1977 there appeared a brief report[6] that $[N(n\text{-}C_4H_9)_4]_2Tc_2Cl_8$ had been prepared, but intensive efforts to reproduce this work have led only to the isolation[7] of compounds containing the $[TcOCl_4]^-$ ion and the alleged existence of the $[Tc_2Cl_8]^{2-}$ ion in a stable crystalline compound remains unconfirmed.

The only ditechnetium(III) compound with a $\sigma^2\pi^4\delta^2$ quadruple bond that has been conclusively isolated and characterized[8] is $Tc_2(O_2CCMe_3)_4Cl_2$, which was shown to have the same paddle-wheel structure (with Tc–Tc = 2.192 (2) Å and Tc–Cl = 2.408 (4) Å) as its rhenium analogue.[9] Unfortunately, this compound is produced in quantities of only 1–5 mg in each preparation, and we have been unable to increase the yield. It is not, therefore, a practical candidate for further investigation, nor is it a practical starting material for other syntheses.

In an effort to explore ditechnetium chemistry further, with the particular hope of perhaps obtaining another compound containing a quadruple bond, we have carried out a reaction between $(NH_4)_3Tc_2Cl_8$ and 2-hydroxypyridine (α-pyridone). The compound $Re_2(OC_5H_4N)_4Cl_2$ had been prepared and characterized shortly before.[10] Again, however, with technetium the compound obtained contains the element in the mixed oxidation state 2.5, with a Tc–Tc bond order of 3.5. The compound is, nonetheless, unusually interesting because of its visible absorption spectrum, which we have measured on single crystals at 5 K.

Experimental Section

Preparation. The starting material, $(NH_4)_3Tc_2Cl_8$, was prepared by a literature method.[1,2] The preparation of $Tc_2(OC_5H_4N)_4Cl$ was conducted using oven-dry glassware and in a nitrogen atmosphere. Transfers were made using standard Schlenk techniques. 2-Hydroxypyridine, 0.50 g, was heated to its melting point and vacuum degassed. To the molten material at 150 °C was added 0.10 g of the ammonium octachloroditechnetate, which upon dissolution produced a dark olive-green solution. After 18 h the color had faded and a dark precipitate was observed. The hot contents of the flask were filtered through a hot frit and, after cooling, the precipitate was washed with CH_2Cl_2 to remove excess hydroxypyridine. The dark green $Tc_2(OC_5H_4N)_4Cl$ was produced in nearly quantitative yield. A small portion of the product was sealed in a 7 × 150 mm Pyrex tube under vacuum (10^{-7} mmHg) and heated in a muffle furnace at 350 °C over a period of 18 h. The furnace was cooled at ~50 °C/h and the tube removed at 80 °C. The walls of the tube were lined with large high-quality crystals.

X-ray Crystallographic Studies.[11,12] Crystals produced by sublimation exhibited strong red-green dichroism, and a small crystal having approximate dimensions of 0.3 × 0.2 × 0.2 mm that was selected for X-ray work exhibited ω-scan half-height widths of less than 0.1° on several low-angle reflections. Intensity data were collected using a CAD-4 automated diffractometer and graphite monochromatized Mo Kα radiation (fine focus tube, 45 kV, 16 mA, take-off angle 2.8°). A random, automatic searching routine located and centered 25 reflections having $20° < 2\theta < 35°$. An indexing routine selected a unit cell of the tetragonal system with the dimensions a = 11.793 (3) Å, c = 7.454 (1) Å, and V = 1036.7 (6) Å^3. The observed volume corresponds to Z = 2 for the expected dinuclear molecule. No systematic absences were observed with the exception of the body-centering condition hkl, $h + k + l = 2n$. A comparison of redundant reflections about the fourfold axis gave $hkl \neq \bar{h}\bar{k}l = h\bar{k}l$, suggesting any of the three space groups $I4$, $I\bar{4}$, or $I4/m$.

Data were collected in the range $0° < 2\theta < 70°$ using the θ–2θ scan mode with a θ scan range of 0.7 + (0.35) tan θ centered on the Mo K$\bar{\alpha}$ intensity maximum. The scan speeds, determined by a 20°/min prescan, varied from 2.5 to 21°/min. The vertical slit was fixed at 4 mm, while the horizontal aperture was varied by (1.5 + tan θ). Three orientation standards monitored every 100 reflections gave no indication of alignment deviation. No linear trends were observed in three reflection intensities monitored after every hour of beam exposure. A total of 1016 reflections having $I > 5\sigma(I)$ were used in the structure refinement.

0002-7863/80/1502-1570$01.00/0

Table I. Positional and Thermal Parameters and Their Estimated Standard Deviations[a]

atom	*x*	*y*	*z*	*B*(1,1)	*B*(2,2)	*B*(3,3)	*B*(1,2)	*B*(1,3)	*B*(2,3)
Tc	0.0000(0)	0.0000(0)	0.14054(7)	1.59(2)	1	1.18(1)	0	0	0
Cl	0.0000(0)	0.0000(0)	0.5000(0)	3.9(2)	3	1.24(7)	0	0	0
O,N	−0.0644(3)	−0.1645(3)	−0.1555(4)	3.0(1)	2.5(1)	2.8(1)	−0.0(1)	−0.63(9)	−0.69(9)
C(1)	−0.0858(5)	−0.2195(5)	0.000(0)	2.1(2)	1.8(2)	4.0(3)	−0.4(2)	0	0
C(2)	−0.1293(7)	−0.3293(7)	0.032(1)	3.2(3)	2.1(2)	4.2(7)	−0.6(2)	0.0(3)	0.2(3)
C(3)	−0.1569(10)	−0.3863(9)	−0.120(2)	3.8(4)	2.7(3)	3.8(4)	−1.1(3)	−0.4(3)	−0.4(3)
C(4)	−0.1443(10)	−0.3359(10)	−0.287(2)	3.9(4)	3.9(4)	4.2(4)	−2.3(3)	−0.4(3)	−1.2(3)
C(5)	−0.0976(8)	−0.2262(9)	−0.296(1)	2.7(3)	3.0(3)	3.1(3)	0.1(3)	−0.4(3)	−0.6(3)

[a] The form of the anisotropic thermal parameter is $\exp[-\frac{1}{4}(B_{11}h^2a^{*2} + B_{22}k^2b^{*2} + B_{33}l^2c^{*2} + 2B_{12}hka^*b^* + 2B_{13}hla^*c^* + 2B_{23}klb^*c^*)]$.

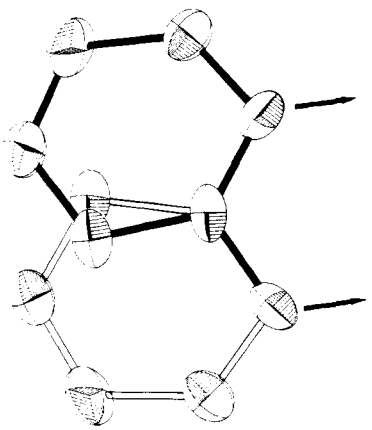

Figure 1. A drawing showing the disorder of the ligand in the model refined.

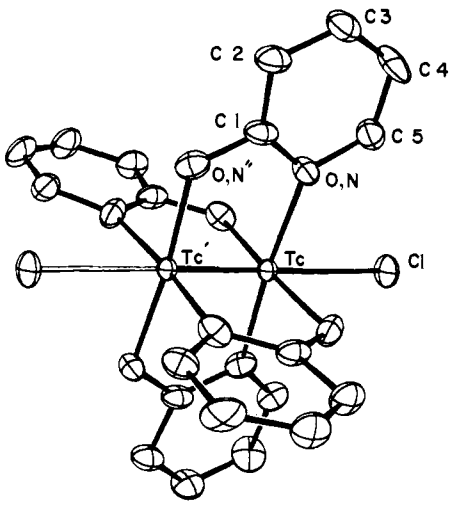

Figure 2. The $Tc_2(OC_5H_4N)_4$ unit and its neighboring Cl atoms. Ellipsoids of thermal vibration are drawn to enclose 40% of the electron density.

The linear absorption coefficient of 14.7 cm^{-1} would ordinarily not indicate that absorption corrections are required. However, the morphology of the crystal was such as to possibly produce some significant intensity errors. Three intense reflections near $\chi = 90°$ were therefore examined at 10° intervals over the range $0° < \psi < 360°$. A plot of the observed intensities about these three diffraction vectors showed only random counting deviations, and the absorption corrections were therefore omitted.

Solution and Refinement of Structure. Statistical tests on the data weakly suggested acentricity and refinement was begun in $I\bar{4}$. The coordinates of the Tc atom were obtained from the Patterson map. One cycle of least-squares refinement on these coordinates gave agreement indices of $R_1 = \Sigma||F_o| - |F_c||/\Sigma|F_o| = 0.41$ and $R_2 = [\Sigma w(|F_o| - |F_c|)^2/\Sigma w|F_o|^2]^{1/2} = 0.51$. The function minimized is $\Sigma w(|F_o| - |F_c|)^2$. The weights, $w = \sigma^{-2}(F_o)$, were derived from $\sigma(F_o) = [\sigma(I_{raw})^2 + (pF_{raw}^2)^2]^{1/2}/Lp$, where $\sigma(I_{raw})$ is based on counting statistics and p is determined by statistical treatment of a cross section of the data. A difference Fourier map revealed the positions for Cl, O, N, and C(1); however, subsequent refinement and difference maps indicated some degree of disorder in the oxopyridinium ring. At this point two ways of continuing the refinement had to be considered. Refinement in $I\bar{4}$ could be continued using a superposition of two nonequivalent orientations which could differ in occupancy, while refinement in $I4/m$ would also be possible using a random disordering of ligand orientations. Since the available resolution would not allow the discernment of O, N, and C(1) atoms for the two orientations, these were treated as full-weighted atoms. The remaining half-weighted C atoms were located and refined in $I\bar{4}$. Refinement of occupation numbers in $I\bar{4}$ gave a result with unequally weighted ligand orientation. Refinement in $I4/m$ with disorder produced lower residuals. Since the latter also seemed more reasonable physically, refinement in the centric space group $I4/m$ was converged for the positional and anisotropic thermal parameters for the eight atoms, producing final residuals of $R_1 = 0.045$ and $R_2 = 0.069$. Failure of this model to account accurately for the density about O, N, and C(1) is probably the main reason for the high estimated standard deviation of an observation of unit weight, 1.58. A final difference map revealed no peaks of structural significance except a few that might have been associated with hydrogen atoms about the ligand ring. In view of the disorder it was considered unjustified to attempt to include these in the refinement. Of the 57 positional and thermal variables, none were found to shift more than 0.4 during the final cycle.

Raman Spectra. Measurements were made on a Cary 82 spectrometer using the 514-nm line of an argon laser. The sample was contained in a 0.5-mm glass capillary.

Mass Spectrum. Measurements were obtained on a CED21-110B high-resolution instrument with a 70-eV ionizing electron beam. The sample probe was maintained at 360°C and the detector at 230 °C. The computer simulation program was supplied by Dr. M. W. Extine.

Crystal Spectra. Spectra were recorded on a Cary 17-D spectrophotometer using equipment previously described.[13] For crystals, two Glan-Thompson polarizers were added, one placed behind the sample and the other in the reference beam. Crystals were mounted over pinholes made in brass foil and were held in place by vacuum grease. Base lines were recorded using identical pinholes as samples and were subtracted from the spectra before plotting.

The crystal morphology was determined by mounting a crystal used for spectroscopy on a goniometer head and indexing it on an Enraf-Nonius CAD-4 automatic diffractometer. Various indices were placed into the diffracting position and the faces noted. Crystal thickness was determined by measurement under a microscope with a calibrated reticule.

Results

Structure. The atomic parameters are listed in Table I. The problem of disorder in the ligand orientations has been discussed in the Experimental Section. The relationship between the two ring positions is shown in Figure 1, where it is seen that three atoms, O, N, and C(1), have positions that are the same for both orientations, except, of course, for the indistinguishability of N and O. Figure 2 shows a drawing of the entire molecule on the arbitrary assumption that the arrangement in each molecule is such as to give D_{2d} symmetry. We cannot rule out C_{2h} symmetry, in which the Tc-N bonds on one metal atom would be cis instead of trans. In truth, our disordered

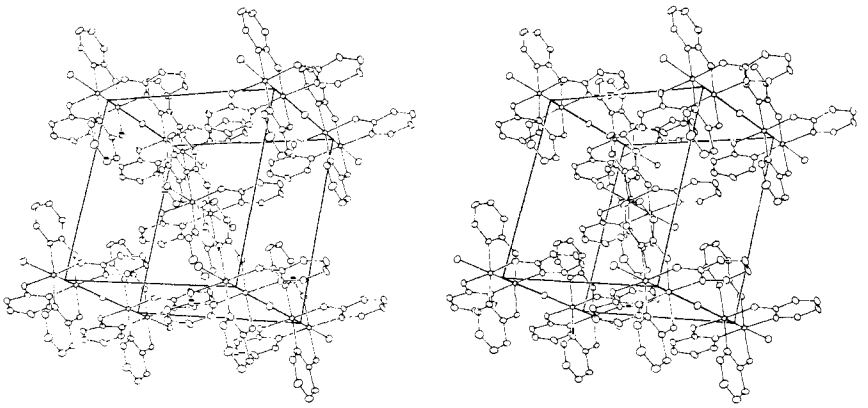

Figure 3. A stereoview of the contents of the unit cell.

Table II. Bond Distances and Angles in $Tc_2(ONC_5H_4)_4Cl$

	Distances (Å)		
Tc-Tc′	2.095(1)	-C(5)	1.332(8)
-Cl	2.679(1)	C(3)-C(2)	1.36(1)
-O,N	2.087(3)	-C(4)	1.38(1)
Cl-O,N	1.532(2)	C(4)-C(5)	1.41(1)
-C(2)	1.412(8)		
	Angles (deg)		
Tc-Tc-Cl	180.00[a]	-C(2)	111.3(5)
-O,N	93.07(7)	C(1)-O,N-C(5)	110.8(5)
Cl-Tc-O,N	86.93(7)	-C(2)-C(3)	113.6(9)
O,N-Tc-O,N	173.8(1)	C(4)-C(5)-O,N	125.3(8)
Tc-O,N-C(1)	117.9(2)	-C(3)-C(2)	120.6(7)
C(5)	131.0(4)	C(3)-C(4)-C(5)	118.7(8)
O,N-C(1)-O,N″	118.1(4)		

[a] Required by symmetry.

model tells nothing about the molecular symmetry. Table II lists the bond distances and angles.

The molecules are packed with normal van der Waals contacts in the x and y directions. In the z direction $Tc_2(OC_5H_4N)_4$ units are arranged in parallel infinite chains with Cl atoms midway between. The Tc-Tc···Cl··· chains lie along the 0, 0, z and the $\frac{1}{2}$, $\frac{1}{2}$, z axes, as shown in the stereoview of the unit cell, Figure 3.

Spectra. The compound is expected to have one unpaired electron per formula unit and an ESR spectrum, kindly run by Dr. T. R. Felthouse, had a strong signal and a g value of 2.046.

A portion of the mass spectrum is shown in Figure 4. It is clear that individual $Tc_2(OC_5H_4N)_4Cl$ molecules pass into the gas phase intact and undergo ionization without dissociation. The pattern is quite simple since the technetium is monoisotopic (^{99}Tc); the peaks at m/e 609 and 611 are due to molecules with ^{35}Cl and ^{37}Cl, respectively, with all other elements (C, N, O, H) present as their major (>99%) isotopes, while the peaks at m/e 610 and 612 are due to those molecules in which one atom of one such element is present as the isotope with a mass number one unit higher, i.e., ^{13}C, ^{15}N, ^{2}H. The complete mass spectrum also contained peaks corresponding to the $Tc_2(OC_5H_4N)_xCl_y^+$ ions with x = 2, 3, 4, and y = 0, 1.

The Raman spectrum, shown in Figure 5, has a very strong, sharp line at 383 cm^{-1} which may be assigned to the totally symmetric mode that is mainly Tc-Tc stretching.

We have also recorded the Raman spectrum of $(NH_4)_3Tc_2Cl_8$ in aqueous solution and this is shown in Figure 6. The band at 370 cm^{-1} may be assigned to the Tc-Tc stretch and the one at 305 cm^{-1} to the totally symmetric Tc-Cl stretching mode.

Electronic absorption spectra are presented in Figures 7-10.

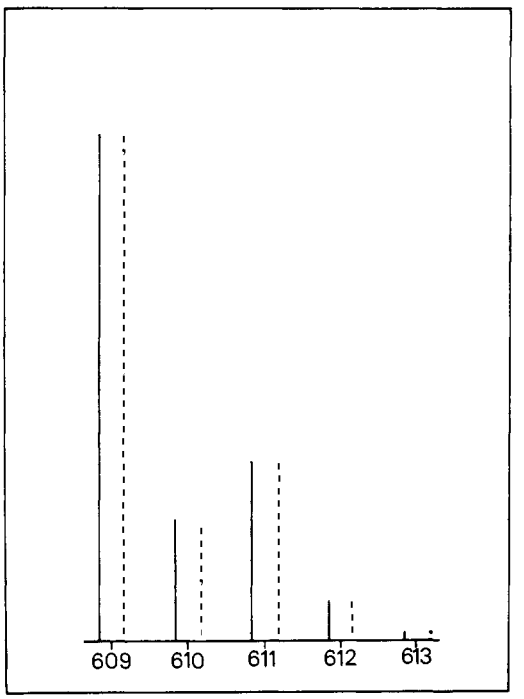

Figure 4. The observed (—) and calculated (- - -) multiplet (m/e) values for the parent ion peak in the mass spectrum of $Tc_2(OC_5H_4N)_4Cl$. The height of each line is proportional to the intensity at that m/e value.

In Figure 8 it must be noted that the noise level due to stray light in the x-y polarized spectrum becomes quite high at frequencies above about 15 000 cm^{-1}; none of the spikes seen above this frequency are genuine spectral features.

Discussion

Structure and Bonding. These require little comment beyond what has already been said. The Tc-Tc distance, 2.095 (1) Å, is the shortest one observed, the others being 2.117 (2) Å in $[Tc_2Cl_8]^{3-}$ and 2.192 (2) Å in $Tc_2(O_2CCMe_3)_4Cl_2$. The slight shortening of the bond on going from $[Tc_2Cl_8]^{3-}$ to the present compound is not surprising since there is a similar shortening for $Mo_2(O_2CR)_4$ compounds ($d_{Mo-Mo} \approx 2.10$ Å) as compared to $[Mo_2Cl_8]^{4-}$ ($d_{Mo-Mo} \approx 2.14$ Å). The rather long bond in $Tc_2(O_2CCMe_3)_4Cl_2$, where the bond order is 4.0, while it is only 3.5 in the present case is probably caused by the relatively short axial Tc-Cl bonds (2.408 (4) Å) in the former as compared to the much longer ones (2.679 (1) Å) in $Tc_2(OC_5N_4N)_4Cl$.

Electronic Absorption Spectrum. The insolubility of $Tc_2(OC_5H_4N)_4Cl$ in all solvents tried made it impossible to record a solution spectrum and, hence, to determine extinction coefficients. The spectrum measured on the powdered com-

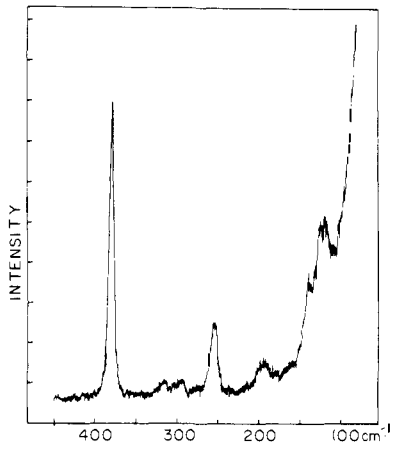

Figure 5. The Raman spectrum of a powdered sample of $Tc_2(OC_5H_4N)_4Cl$. Excitation: 514.6 nm with 10-mW power at sample surface.

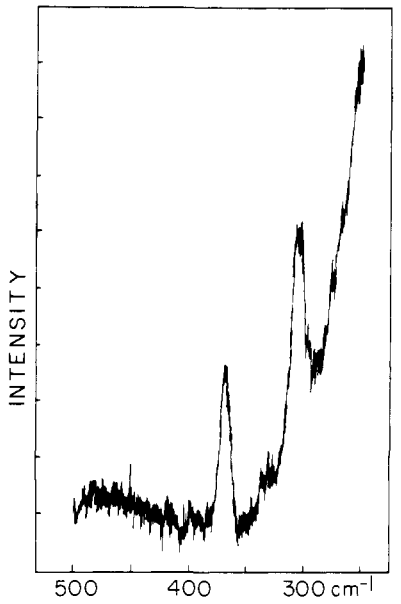

Figure 6. The Raman spectrum of $(NH_4)_3Tc_2Cl_8$ in 12 M hydrochloric acid solution. Excitation: 514.6 nm.

pound in a KBr disk is shown in Figure 7. At room temperature the broad, intense band at 25 000 cm^{-1} is the only feature resolved. At 5 K, however, weak bands centered at 13 000, 17 000, and 18 000 cm^{-1} were observed. Neither in the KBr disk nor in the spectra of single crystals was any absorption band observed in the near-infrared region. The band at about 13 000 cm^{-1} is evidently the lowest energy electronic transition for this compound.

Spectra recorded in the (1,1,0) face of a single crystal at 5 K are shown in Figure 8. In this tetragonal crystal the molecular axes are perfectly aligned with the crystal axes and *c* polarization for the crystal is identical with *z* (metal-metal) polarization for the molecule. The crystal used was wedge shaped with a minimum thickness of 50 μm. An upper limit of the molar absorptivity can be found by multiplying the absorbance by 62.4 M^{-1} cm^{-1}. The bands observed in the crystal, therefore, are quite weak.

The spectrum of the isoelectronic $[Tc_2Cl_8]^{3-}$ ion has been reported and assigned previously.[4] The transitions were assigned with guidance from an SCF-Xα-SW calculation.[5] There was excellent agreement between the observed and calculated transitions. In $Tc_2Cl_8^{3-}$ the lowest energy feature was a 0-0 transition at 5900 cm^{-1}, with a molar absorptivity of 630 M^{-1} cm^{-1}. In a KBr pellet, vibrational structure was

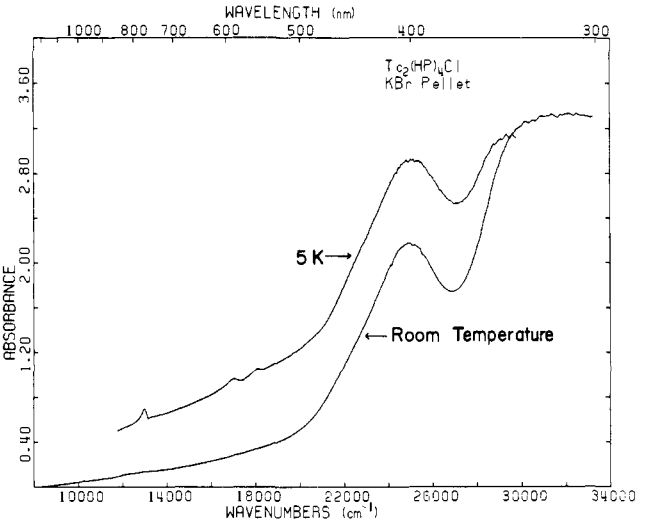

Figure 7. The spectrum of $Tc_2(OC_5H_4N)_4Cl$, powdered and pressed in a KBr disk.

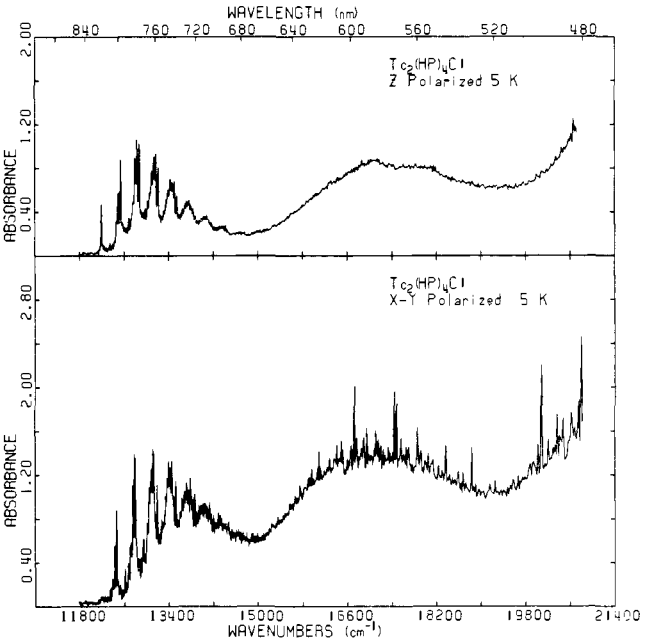

Figure 8. Polarized spectra in the (1,1,0) face of a single crystal of $Tc_2(OC_5H_4N)_4Cl$ at 5 K, drawn from data points every 0.1 nm.

observed even at room temperature and at 5 K a mean separation of 320 cm^{-1} was measured. This band was assigned as the $^2B_{2g} \leftarrow {}^2B_{1u}$ ($\delta^* \leftarrow \delta$) transition, and the vibrational quantum of 320 cm^{-1}, which represents Tc-Tc stretching in the excited state, is about 50 cm^{-1} lower than the frequency of the band in the ground-state Raman spectrum that is assigned to the same type of stretching mode. This magnitude of reduction in ν_{M-M} from the ground state to an excited state obtained by $\delta^* \leftarrow \delta$ excitation is reasonable and consistent with results on other systems[9] such as $[Mo_2Cl_8]^{4-}$, $Mo_2(O_2CR)_4$, and $[Re_2Cl_8]^{2-}$.

The lowest energy band in $Tc_2(OC_5H_4N)_4Cl$, centered around 13 000 cm^{-1}, is seen in the low-temperature crystal spectra of Figure 8 to have a 0-0 line at 12 194 cm^{-1} that is completely *z* polarized. This clearly supports the assignment of the band to the $\delta^* \leftarrow \delta$ transition and leads to the conclusion that there is a hypsochromic shift of about 6300 cm^{-1} from $[Tc_2Cl_8]^{3-}$ to $Tc_2(OC_5H_4N)_4Cl$. This shift is about twice as large as the one from $[Mo_2Cl_8]^{4-}$ to the $Mo_2(O_2CR)_4$ compounds.[15]

The next two bands in $Tc_2Cl_8^{3-}$ were at 13 600 (ϵ 35) and

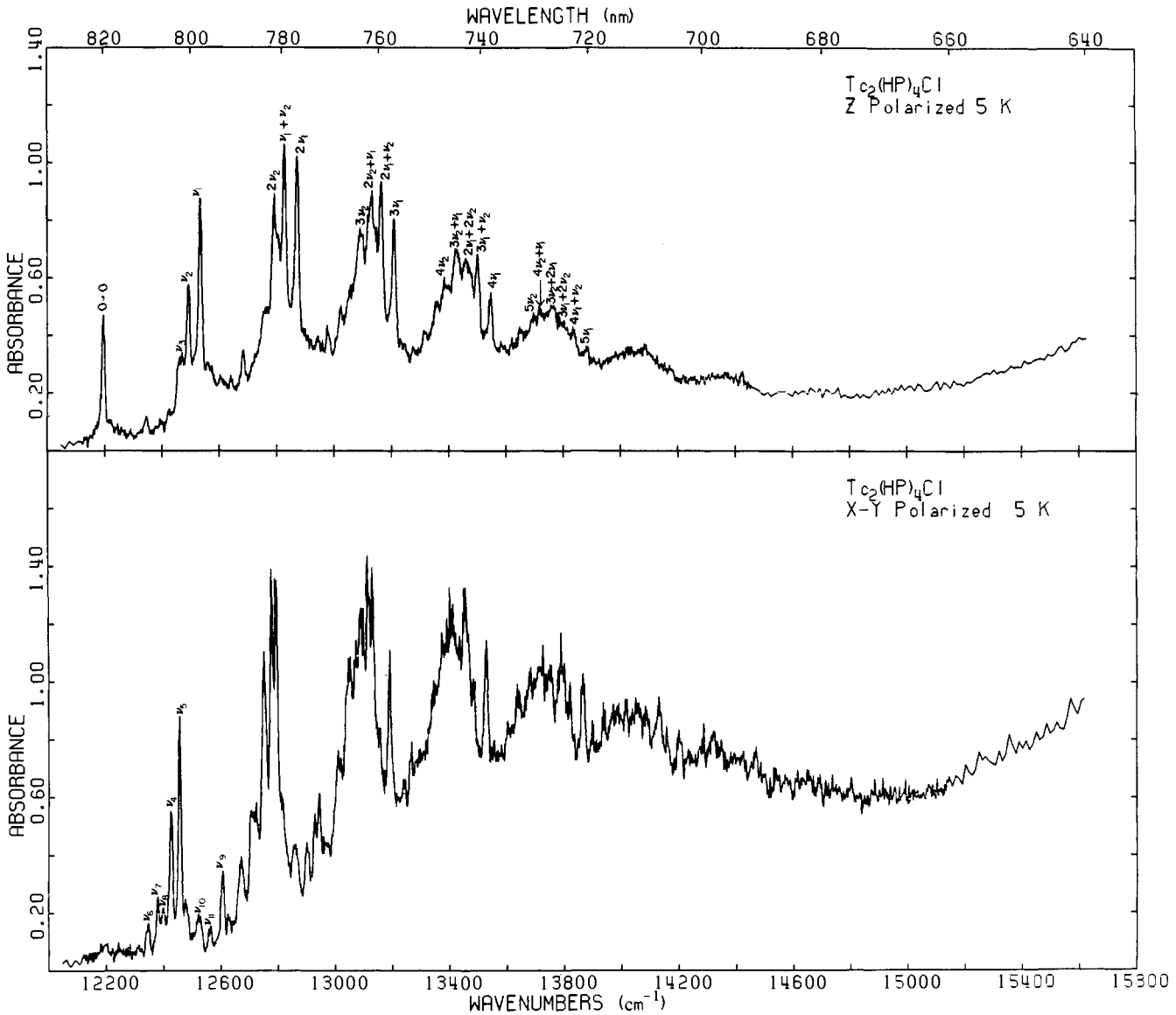

Figure 9. Polarized crystal spectrum of the $\delta^* \leftarrow \delta$ transition of $Tc_2(OC_5H_4N)_4Cl$ at 5 K, drawn from data points every 0.1 nm.

15 700 cm^{-1} (ϵ 172) and were assigned as $^2E_u \leftarrow {}^2B_{1u}$ ($\delta^* \leftarrow \pi$) and $^2E_g \leftarrow {}^2B_{1u}$ ($\pi^* \leftarrow \delta^*$), respectively. The weakness of the $\delta^* \leftarrow \pi$ transition can be attributed simply to its being Laporte forbidden in D_{4h} symmetry. Although the $\pi^* \leftarrow \delta^*$ transition is fully allowed, the extinction coefficient of 172 M^{-1} cm^{-1} indicates that it is quite weak. The transitions at 17 000 and 18 000 cm^{-1} are presumed to be the corresponding transitions in $Tc_2(OC_5H_4N)_4Cl$. These transitions are broad and quite weak, and it was not possible to obtain definitive polarization data from the crystal spectrum. This is because they derive intensity from vibronic coupling which can provide intensity in the polarization opposite to that calculated for the transition moment. Furthermore, vibronic coupling can break down the oriented gas assumption. In any case, the feature at 17 100 cm^{-1} is the more intense of the two and is therefore assigned as the $\pi^* \leftarrow \delta^*$ transition. Its intensity here is comparable to that in $[Tc_2Cl_8]^{3-}$. The band at 18 000 cm^{-1} is the $\delta^* \leftarrow \pi$ transition. This is the reverse of the assignment in $[Tc_2Cl_8]^{3-}$ but is not unreasonable in view of the greater separation between the δ and δ^* orbitals observed for $Tc_2(OC_5H_4N)_4Cl$. The effect of raising the δ^* orbital would be to increase the π-δ^* separation and decrease the δ^*-π^* separation as observed. The next weak feature in $[Tc_2Cl_8]^{3-}$ was observed at 20 000 cm^{-1} (ϵ 10). No similar feature was observed in $Tc_2(OC_5H_4N)_4Cl$ because the region is masked by the intense band at 25 000 cm^{-1}.

The first intense transition in $[Tc_2Cl_8]^{3-}$, assigned as either $\delta^* \leftarrow Cl(\pi)$ or the $\pi^* \leftarrow \pi$ transition, was at 31 400 cm^{-1} (ϵ 3900). It seems unlikely in view of the greater δ-δ^*, δ^*-π^*, and π-δ^* separations that the transition at 25 100 cm^{-1} in $Tc_2(OC_5H_4N)_4Cl$ is a bathochromically shifted $\pi^* \leftarrow \pi$ transition. Therefore, it is assigned as a $\delta^* \leftarrow L(\pi)$ transition. This transition would be expected at a lower energy than in the chloride complex because the hydroxypyridine π system should be at higher energy and hence closer in energy to the metal-metal orbitals.

The lowest energy band, commencing at 12 194 cm^{-1} in the crystal, displays a plethora of vibrational structure at 5 K. The lowest energy feature is purely z (c) polarized and is assigned as the 0-0 transition. This transition is reminiscent of the weak $\delta^* \leftarrow \delta$ transition observed in $Mo_2(O_2CCH_3)_4$. In both cases, the transition is fundamentally z polarized but it is overlaid with components of equal or greater intensities having x-y polarization. The x-y intensity arises from the vibronic coupling of various modes corresponding to those that would be e_g modes in full D_{4h} symmetry. The vibronic intensity is then as great as the dipole-allowed intensity. In addition, a variety of polarization ratios is observed. This is because of the

Table III. Vibrational Structure Observed in the $\delta^* \leftarrow \delta$ Transition in $Tc_2(OC_5H_4N)_4Cl$

λ, nm	ν, cm^{-1}	polarization (comment)	assignment	λ, nm	ν, cm^{-1}	polarization (comment)	assignment
820.1	12 194.4	*z*	0-0	734.4	13 617.5	*xy*	$\nu_4 + 4\nu_2$
810.1	12 344.2	*z–xy*	ν_6	733.5	13 633.3	*xy*	$\nu_9 + 3\nu_1$
807.8	12 379.3	*xy*	ν_7	732.6	13 650.9	*z*	$\nu_2 + 4\nu_1$
806.5	12 399.3	*xy*	ν_8	732.3	13 655.6	*xy* (broad)	$\nu_4 + \nu_1 + 3\nu_2$; $\nu_5 + 4\nu_2$
804.8	12 425.4	*xy–z*	ν_4	731.3	13 675.2	*z* (broad)	$5\nu_2$; $\nu_3 + 3\nu_2 + \nu_1$
802.7	12 457.9	*z*	ν_3	730.3	13 693.0	*xy*	$\nu_4 + 2\nu_1 + 2\nu_2$; $\nu_5 + 3\nu_2 + \nu_1$; $\nu_6 + 4\nu_1$
802.0	12 469.6	*xy*	ν_5				
800.5	12 493.0	*z*	ν_2	729.0	13 717.4	*z* (broad)	$4\nu_2 + \nu_1$; $\nu_3 + 2\nu_1 + 2\nu_2$
797.9	12 533.7	*z*	ν_1	728.6	13 725.0	*xy*	$\nu_{10} + 4\nu_2$
797.7	12 536.0	*xy*	ν_{10}	727.8	13 741.0	*xy*	$\nu_4 + 3\nu_1 + \nu_2$; $\nu_5 + 2\nu_1 + 2\nu_2$
796.3	12 558.1	*z* (broad)	phonon structure				
795.3	12 574.7	*xy*	ν_{11}	726.6	13 763.6	*z*	$3\nu_2 + 2\nu_1$; $\nu_2 + 3\nu_3 + \nu_1$
792.5	12 619.9	*xy*	ν_9	726.5	13 764.6	*xy* (broad)	$\nu_4 + 4\nu_1$; $\nu_{10} + 3\nu_2 + \nu_1$
791.1	12 640.6	*xy*	$\nu_6 + \nu_2$	725.4	13 786.4	*xy*	$\nu_5 + 3\nu_1 + \nu_2$
778.4	12 684.7	*xy*	$\nu_6 + \nu_1$	724.6	13 800.7	*z* (broad)	$2\nu_2 + 3\nu_1$; $4\nu_1 + \nu_3$
787.6	12 696.8	*xy*	$\nu_8 + \nu_2$	724.3	13 807.4	*xy*	$\nu_{10} + 2\nu_2 + 2\nu_1$
786.1	12 721.0	*xy*	$\nu_4 + \nu_2$; $\nu_7 + \nu_1$	723.6	13 819.8	*xy*	$\nu_5 + 4\nu_1$
785.3	12 734.8	*xy*	$\nu_8 + \nu_1$	722.8	13 835.1	*z*	$\nu_2 + 4\nu_1$
783.5	12 763.2	*z* (broad)	$\nu_3 + \nu_2$	720.4	13 882.1	*z–xy*	$5\nu_1$ $\nu_{10} + 4\nu_1$; $\nu_9 + 2\nu_1 + 2\nu_2$
783.4	12 764.7	*xy*	$\nu_4 + \nu_1$				
781.8	12 791.8	*z, xy*	$2\nu_2$; $\nu_5 + \nu_2$	718.6	13 915.9	*xy* (broad)	$\nu_4 + 5\nu_2$
780.8	12 808.2	*xy*	$\nu_5 + \nu_1$	716.5	13 956.7	*xy*	$\nu_5 + \nu_1 + 4\nu_2$; $\nu_5 + 5\nu_2$
779.6	12 827.9	*z*	$\nu_1 + \nu_2$	715.0	13 986.0	*z*	$6\nu_2$
779.4	12 831.2	*xy*	$\nu_{10} + \nu_2$	714.9	13 988.0	*xy* (shoulder)	$\nu_4 + 2\nu_1 + 3\nu_2$
776.9	12 872.5	*z*	$2\nu_1$	714.2	14 002.7	*xy*	$\nu_5 + \nu_1 + 4\nu_2$
776.7	12 875.0	*xy*	$\nu_{10} + \nu_1$	712.8	14 029.2	*xy*	$\nu_4 + 3\nu_1 + 2\nu_2$; $\nu_5 + 2\nu_1 + 3\nu_2$; $\nu_{10} + 5\nu_2$
774.3	12 915.7	*xy*	$\nu_9 + \nu_2$				
772.8	12 940.8	*xy*	$\nu_6 + 2\nu_2$	711.1	14 062.7	*xy*	$\nu_{10} + 4\nu_2 + \nu_2$
771.8	12 957.6	*xy*	$\nu_9 + \nu_1$	710.3	14 077.6	*xy* (broad)	$\nu_4 + 4\nu_1 + \nu_2$; $\nu_5 + 3\nu_1 + 2\nu_2$
770.0	12 987.0	*xy* (broad)	$\nu_6 + \nu_1 + \nu_2$				
767.9	13 022.5	*xy* (shoulder)	$\nu_4 + 2\nu_2$; $\nu_6 + 2\nu_1$	709.1	14 102.4	*xy*	$\nu_4 + 5\nu_1$; $\nu_{10} + 3\nu_2 + 2\nu_1$
767.5	13 029.3	*xy* (broad)	$\nu_6 + 2\nu_1$	709.0	14 104.7	*z*	$3\nu_2 + 3\nu_1$
766.0	13 054.8	*z*	$\nu_3 + 2\nu_2$	707.8	14 129.3	*xy* (shoulder)	$\nu_5 + 4\nu_1 + \nu_2$
765.7	13 059.9	*xy*	$\nu_4 + \nu_1 + \nu_2$	706.8	14 148.3	*xy*	$\nu_5 + 5\nu_1$; $\nu_{10} + 3\nu_1 + 2\nu_2$
765.2	13 068.5	*xy*	$\nu_5 + 2\nu_2$; $\nu_8 + 2\nu_1$	705.7	14 170.3	*z*	$5\nu_1 + \nu_2$
764.0	13 089.0	*z–xy*	$3\nu_2$; $\nu_4 + 2\nu_1$	705.5	14 174.3	*xy*	$\nu_{10} + 4\nu_1 + \nu_2$
763.5	13 097.6	*z*	$\nu_3 + \nu_2 + \nu_1$	703.3	14 219.7	*xy*	$\nu_{10} + 5\nu_1$
763.1	13 104.4	*xy*	$\nu_5 + \nu_1 + \nu_2$	699.5	14 295.7	*xy*	$\nu_4 + 2\nu_1 + 4\nu_2$; $\nu_4 + \nu_1 + 5\nu_2$
761.7	13 129.4	*z–xy*	$2\nu_2 + \nu_1$; $\nu_{10} + 2\nu_2$				
760.8	13 144.1	*xy*	$\nu_5 + 2\nu_1$	698.1	14 324.6	*xy* (shoulder)	$\nu_4 + 3\nu_1 + 3\nu_2$; $\nu_{10} + 6\nu_2$
759.6	13 164.8	*z*	$2\nu_1 + \nu_2$	697.5	14 336.9	*xy*	$\nu_5 + 2\nu_1 + 4\nu_2$
759.5	13 166.6	*xy* (shoulder)	$\nu_{10} + \nu_1 + \nu_2$	696.0	14 367.8	*xy* (shoulder)	$\nu_4 + 4\nu_1 + 2\nu_2$, $\nu_{10} + 5\nu_2 + \nu_1$
757.3	13 205.7	*xy*	$\nu_9 + 2\nu_2$; $\nu_{10} + 2\nu_1$				
757.1	13 208.3	*z*	$3\nu_1$	694.5	14 398.8	*xy*	$\nu_{10} + 4\nu_2 + 2\nu_1$
754.5	13 253.8	*xy*	$\nu_9 + \nu_1 + \nu_2$	693.9	14 412.3	*xy*	$\nu_4 + 5\nu_1 + \nu_2$; $\nu_5 + 4\nu_1 + 2\nu_2$
753.0	13 280.2	*xy*	$\nu_6 + 2\nu_2 + \nu_1$				
752.1	13 296.1	*xy*	$\nu_9 + 2\nu_1$	690.4	14 485.4	*xy* (broad)	$\nu_{10} + 4\nu_1 + 2\nu_2$
750.4	13 327.1	*xy*	$\nu_6 + 2\nu_1 + \nu_2$	689.1	14 511.7	*xy* (shoulder)	$\nu_{10} + 5\nu_1 + \nu_2$; $\nu_4 + 7\nu_2$
748.4	13 362.7	*xy*	$\nu_4 + \nu_1 + 2\nu_2$; $\nu_5 + 3\nu_2$; $\nu_6 + 3\nu_1$	687.0	14 557.1	*xy*	$\nu_{10} + 6\nu_1$; $\nu_4 + 6\nu_2 + \nu_1$; $\nu_5 + 7\nu_1$
747.0	13 386.7	*z*	$4\nu_2$	685.5	14 587.9	*xy* (broad)	$\nu_4 + 5\nu_2 + 2\nu_1$; $\nu_5 + 6\nu_2 + \nu_1$
746.8	13 390.5	*xy*	$\nu_4 + 2\nu_1 + \nu_2$				
746.0	13 404.8	*xy*	$\nu_5 + \nu_1 + 2\nu_2$	683.5	14 630.6	*xy*	$\nu_4 + 4\nu_2 + 3\nu_1$; $\nu_5 + 5\nu_2 + \nu_1$
744.9	13 424.6	*z–xy*	$3\nu_2 + \nu_1$; $\nu_{10} + 3\nu_2$				
744.3	13 436.3	*xy*	$\nu_4 + 3\nu_2$	681.7	14 669.2	*xy*	$\nu_4 + 4\nu_1 + 3\nu_2$; $\nu_5 + 4\nu_2 + 3\nu_1$
742.9	13 461.7	*z* (broad)	$2\nu_2 + \nu_1$; $\nu_3 + 3\nu_1$				
742.7	13 464.4	*xy*	$\nu_{10} + 2\nu_2 + \nu_1$	680.0	14 705.9	*xy*	$\nu_4 + 5\nu_1 + 2\nu_2$; $\nu_5 + 4\nu_1 + 3\nu_2$
741.8	13 480.7	*xy* (shoulder)	$\nu_5 + 3\nu_1$				
740.9	13 497.1	*xy*	$\nu_{10} + 2\nu_1 + \nu_2$	677.5	14 760.1	*xy* (very broad)	$\nu_5 + 5\nu_1 + 2\nu_2$
740.8	13 499.8	*z*	$3\nu_1 + \nu_2$	674.8	14 820.3	*xy*	$\nu_5 + 7\nu_1$
738.4	13 542.7	*xy*	$\nu_{10} + 3\nu_1$	671.3	14 897.6	*xy*	$\nu_{10} + 7\nu_1$
738.3	13 545.5	*z*	$4\nu_2$	666.3	15 009.4	*xy*	$\nu_5 + 4\nu_1 + 4\nu_2$
736.8	13 572.2	*xy*		659.6	15 160.7	*xy*	$\nu_5 + 8\nu_1$

breakdown of the oriented gas assumption for vibronic transitions.[15] As demonstrated previously[13,15] even the *z*-polarized, dipole-allowed components may gain intensity by Herzberg–Teller coupling. This will alter the Franck–Condon factors and may alter the direction of the transition moment, producing some intensity in the *x–y* polarization. All of these factors must be taken into account in assigning this weak dipole-allowed transition.

The difficulties in making an assignment of all the components of this band are further increased by the fact that the true symmetry of $Tc_2(OC_5H_4N)_4Cl$ is unknown because of the disorder in the crystal structure. As suggested earlier, it is likely

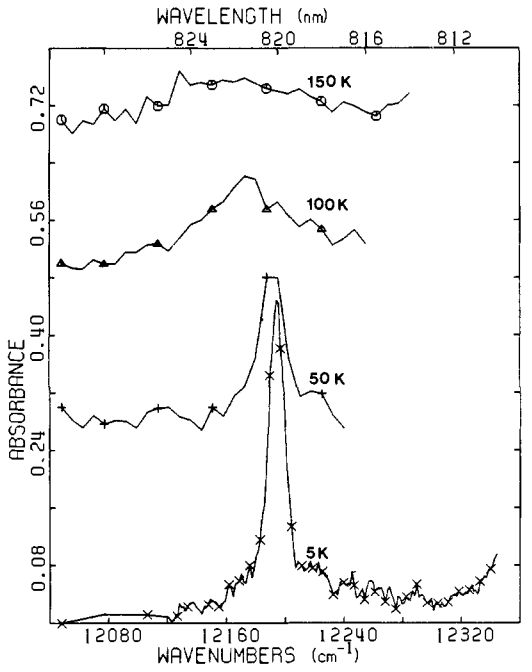

Figure 10. The 0-0 transition for the $\delta^* \leftarrow \delta$ transition of $Tc_2(OC_5H_4N)_4Cl$ as a function of temperature. Crosses denote every fifth data point.

that the local symmetry of the $Tc_2(OC_5H_4N)_4$ unit is either C_{2h} or D_{2d}. The fact that the 0-0 line in the spectrum is sharp and unique strongly supports the idea that all such units are identical in local structure, but does not help to decide which is correct. We shall analyze this band in a way that does not require (or imply) a definite choice of local symmetry.

Three vibrations are seen in the z-polarized spectrum and it seems reasonable to assume that these correspond to Tc-O and Tc-N stretching (264 and 298 cm^{-1}, not necessarily in that order) and Tc-Tc stretching (339 cm^{-1}, which is, very reasonably, about 44 cm^{-1} less than the Tc-Tc stretching frequency in the ground state). Beyond this, however, we see here for the first time in a square prismatic M_2 complex vibrational progressions based on two vibrations and on their combination tones. The two vibrations are ν(Tc-Tc), as expected, and the ν(Tc-L) mode with a frequency of 298 cm^{-1} which is probably the ν(Tc-N) mode. It is then possible to account in complete detail for the continuous increase in the number of peaks in each group as the energy increases. Thus, in the second group we have not only $2\nu_1$ and $2\nu_2$ but $\nu_1 + \nu_2$, while in the third group we have four triple excitations, $3\nu_1$, $3\nu_2$, $2\nu_1 + \nu_2$, and $\nu_1 + 2\nu_2$. The continuation of this pattern is shown in Figure 9 for the next two groups, beyond which low intensity and lack of resolution make it impossible to identify the individual components. The frequencies of all these vibrational lines are listed in Table III. The observation of exactly the right number of combination bands in every group, at exactly the expected frequencies, rules out the possibility that there might be an explanation in terms of difference ν(Tc-Tc) progressions built on different 0-0 bands.

It is very hard to obtain accurate Franck-Condon factors from the observed spectra because the overlap of peaks makes determination of their intensities difficult. Furthermore, the spectral bandwidth was only 0.3 nm or less while the spectra were recorded, which means that the apparent intensities of these narrow features cannot be considered quantitatively reliable. However, it appears that the progression based on ν(Tc-Tc) maximizes in the third member, as in the case of $Mo_2(O_2CCH_3)_4$.[15] The change in bond distance between the ground and excited state was estimated to be 0.1 Å for that case. The Franck-Condon factors for the ν(Tc-L) progression

Table IV. Vibrational Frequencies

mode	symmetry	ν, cm^{-1} (ground state)	ν, cm^{-1} (excited state)	assignment
ν_1	a_1	383	337	Tc-Tc
ν_2	a_1	319	298	Tc-N,O
ν_3	a_1	295	264	Tc-O,N
ν_4		258 broad	231	Tc-O,N
ν_5		258	275	Tc-N,O
ν_6		148	152.8	
ν_7		200 broad	184.9	
ν_8		200	204.9	
ν_9			425.5	
ν_{10}			342	
ν_{11}			380.3	

seem to be less regular. This irregularity, coupled with the fact that these vibrations appear weakly in x-y polarization, indicates that Herzberg-Teller coupling via a totally symmetric vibration is providing some intensity, as in the previously reported cases of $Mo_2(O_2CCH_3)_4$[15] and $Mo_2[(CH_2)_2P(CH_3)_2]_4$.[13] The observation of a Franck-Condon progression based on ν(Tc-L) requires that there must be a significant change in the Tc-L bond distance between the ground and excited electronic states. Further, the frequency of 298 cm^{-1} is presumably the excited-state value for the same vibration that has a frequency of 319 cm^{-1} in the ground state. This means that the electronic transition causes a weakening of the Tc-L bonds concerned. This, in turn, would indicate that the δ orbital has some Tc-L bonding character, which is likely to be connected with Tc-N(π) bonding, with the δ^* orbital having, similarly, some Tc-N(π) antibonding character. This metal-ligand π bonding does not appreciably change the metal-metal bond.

Assignment of the $b(xy)$-polarized spectrum is inherently more difficult, and the difficulties are exacerbated by uncertainty about the molecular symmetry. The following suggestions are therefore tentative. If we were dealing with D_{4h} symmetry, the vibrations observed would all have to be of e_g type to provide x-y intensity for the z-polarized, dipole-allowed transition. In $Tc_2(OC_5H_4N)_4Cl$, the required vibrations must belong to the corresponding representations of either D_{2d} or C_{2h}. Table IV lists observed vibrational frequencies and some possible assignments. The two most intense features, ν_4 and ν_5, are the appropriate non-totally symmetric Tc-O and Tc-N stretching modes. Again, both ν(Tc-Tc) and one of the totally symmetric ν(Tc-L) modes and their combinations are observed as Franck-Condon progressions originating at each pseudoorigin. The frequencies ν_6, ν_7, and ν_8 presumably represent various bending modes but cannot be assigned with confidence. The feature labeled ν_{10} has a frequency of 342 cm^{-1}, which is quite similar to the 339 cm^{-1} for the Tc-Tc stretch. However, the intensity of the progression based on ν_{10} is quite different from the intensity at the corresponding wavelengths in the z-polarized spectrum and therefore ν_{10} cannot be a component of ν_1.

The appearance of the 0-0 band at various temperatures is shown in Figure 10. By 150 K this line has broadened so much that it has disappeared into the base line. This is identical with the temperature behavior of the entire $\delta^* \leftarrow \delta$ band in the KBr pellet spectrum. Such a temperature effect is probably caused by broadening from extensive coupling to phonon bands that are populated at very low temperatures. The disorder and also the chain structure of the crystal may enhance such couplings.

Acknowledgments. We thank the National Science Foundation for financial support.

Supplementary Material Available: A table of observed and calculated structure factors (5 pages). Ordering information is given on any current masthead page.

References and Notes

(1) Eakens, J. D.; Humphreys, D. G.; Mellish, C. E. *J. Chem. Soc.* **1963**, 6012.
(2) (a) Cotton, F. A.; Bratton, K. W. *J. Am. Chem. Soc.* **1965**, *87*, 921. (b) Bratton, W. K.; Cotton, F. A. *Inorg. Chem.* **1970**, *9*, 789. (c) Cotton, F. A.; Shive, L. W. *Ibid.* **1975**, *14*, 2032.
(3) Cotton, F. A.; Pederson, E. *Inorg. Chem.* **1975**, *14*, 383.
(4) Cotton, F. A.; Fanwick, P. E.; Gage, L. D.; Kalbacher, B. J.; Martin, D. S. *J. Am. Chem. Soc.* **1977**, *99*, 5642.
(5) Cotton, F. A.; Kalbacher, B. J. *Inorg. Chem.* **1977**, *16*, 2386.
(6) Schwochau, K.; Hedwig, K.; Schenk, H. J.; Greis, O. *Inorg. Nucl. Chem. Lett.* **1977**, *13*, 77.
(7) Cotton, F. A.; Davison, A.; Day, V. W.; Gage, L. D.; Trop, H. S. *Inorg. Chem.* **1979**, *18*, 3024.
(8) Cotton, F. A.; Gage, L. D. *Nouveau J. Chim.* **1977**, *1*, 441.
(9) Collins, D. M.; Cotton, F. A.; Gage, L. D. *Inorg. Chem.* **1979**, *18*, 1712.
(10) Cotton, F. A.; Gage, L. D. *Inorg. Chem.* **1979**, *18*, 1716.
(11) Procedures for data collection and data reduction with the CAD-4 diffractometer have been described earlier: Bino, A.; Cotton, F. A.; Fanwick, P. E. *Inorg. Chem.* **1979**, *18*, 3558.
(12) All computing to solve and refine the structure was carried out on a PDP 11/45 computer at the Molecular Structure Corp., College Station, Tex., using the Enraf-Nonius structure determination package with some local modifications.
(13) Cotton, F. A.; Fanwick, P. E. *J. Am. Chem. Soc.* **1979**, *101*, 5252.
(14) Fanwick, P. E.; Martin, D. S.; Cotton, F. A.; Webb, T. R. *Inorg. Chem.* **1977**, *16*, 2103.
(15) Martin, D. S.; Newman, R. A.; Fanwick, P. E. *Inorg. Chem.* **1979**, *18*, 2511.

Unsaturated Acyl Derivatives of Silicon, Germanium, and Tin from Metalated Enol Ethers[2a]

John A. Soderquist[1a] and Alfred Hassner*[1b]

Contribution from the Department of Chemistry, State University of New York at Binghamton, Binghamton, New York 13901.

Received July 2, 1979

Abstract: The preparation of 1-lithio derivatives of some conjugated vinyl ethers is described. Reaction of these compounds with the chlorotrimethyl derivatives of silicon, germanium, and tin gives the corresponding metallovinyl ethers in 50–80% yield. At least in the case of silicon these reactions proceed with retention of stereochemistry. The silyl compounds undergo $Z \rightleftharpoons E$ photoisomerization. Hydrolysis of the ethers in aqueous acetone gives the corresponding acylmetallanes in 60–75% yield. The metalation and hydrolysis reactions are examined in some detail. The spectral properties of these novel unsaturated acylmetallanes are presented and discussed.

Introduction

Studies in our laboratory have revealed that 1-trimethylsilylacetylenes can be converted to the corresponding α-silaketones (acylsilanes) using a hydroboration/oxidation sequence.[2b] From the enyne **1**, it was possible to prepare the first example of an acrylic α,β-unsaturated acylsilane (**3**) since the oxidation of the vinylboronate (**2**) is accompanied by isomerization of the double bond into conjugation (eq 1). In spite of

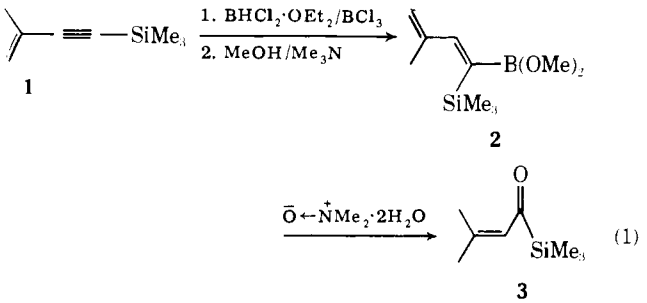

1 2 3 (1)

repeated attempts, we were unable to extend this method to the preparation of the corresponding germanium and tin ketones. Under our conditions, the hydroboration step failed to give the desired adducts, presumably owing to the strong Lewis acid nature of the reactants. Therefore, we chose to investigate other routes to **3**, which could accommodate not only a variety of enone moieties, but also germanium and tin substitution.

To date, the most convenient and general methods for the preparation of acyl derivatives of silicon and germanium involve the use of masked acyl anion equivalents,[3] including the dithiane method.[4] Unfortunately, this method fails in the hydrolysis step for the tin case.[4]

More recently, Baldwin and co-workers have reported that lithiated 1-methoxybutadiene can be used as a crotonyl anion equivalent.[5] Owing to the exceptionally mild conditions required to hydrolyze vinyl ethers, an approach to α,β-unsaturated acylmetallanes based on such compounds seemed particularly attractive. Therefore, we undertook an investigation of the metalation of several representative vinyl ethers and their conversion to acylmetallanes.

Results and Discussion

Synthesis and Photochemistry of Metalated Enol Ethers. When *trans*-1-methoxy-1,3-butadiene was metalated using 1 equiv of *tert*-butyllithium and the resulting 1-lithiated compound (**5**) was treated with the chlorotrimethyl derivatives of silicon, germanium, and tin, the corresponding adducts (**6**) (eq 2) were isolated in good yields.

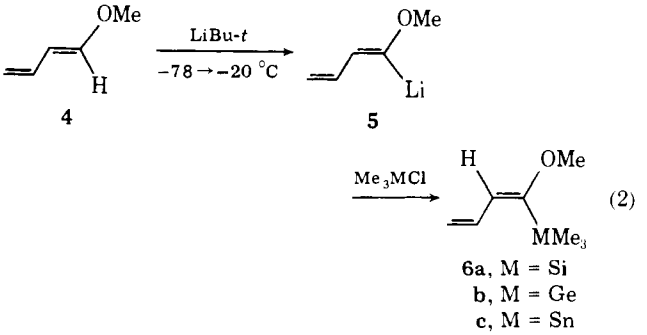

4 5

6a, M = Si
b, M = Ge
c, M = Sn (2)

Minor amounts (<5%) of *trans*-1 methoxy-5,5-dimethylhex-2-ene (**7**) were formed in each case, apparently arising from the addition of *tert*-butyllithium to **4**.

Photoisomerization of the silylated ether (**6a**) in C_6D_6 (monitored by GC) led to a photostationary 60:40 mixture of

0002-7863/80/1502-1577$01.00/0